Revista Brasileira de Meteorologia, 11(1/2): 6-17, 1996

TROPICAL CIRCULATION VARIABILITY WITH EMPHASIS ON INTERANNUAL AND INTRASEASONAL TIME SCALES

MARY T. KAYANO
Instituto Nacional de Pesquisas Espaciais
Departamento de Ciências Meteorológicas
C.P. 515, CEP: 12227-010, São José dos Campos, SP, Brazil

VERNON E. KOUSKY
National Centers for Environmental Prediction
Climate Prediction Center
Washington, D.C., 20233, USA

ABSTRACT

Tropical atmosphere variability is analyzed by computing the variance (total, interannual - IA, and intraseasonal - IS) of outgoing longwave radiation (OLR), sea level pressure (SLP), 250-hPa streamfunction and 250-hPa velocity potential, and the percent of total variance in the IA and IS bands, for the period 1985-1994 for all seasons and for the austral summer and winter seasons, separately. High OLR variability in the tropics and subtropics is mainly associated with the IS band, whereas the maximum IA variance observed in the equatorial central and eastern Pacific is related to the El Niño-Southern Oscillation (ENSO). The SLP variance is largest in the extratropics, however, the pattern of percent of total variance in the IA band shows maxima in the tropics consistent with the centers of action of the Southern Oscillation (SO). A substantial portion of the IS variance in SLP is related to the Madden-Julian oscillation. The greatest variance of the 250-hPa streamfunction is found in the subtropics and lower midlatitudes. The small regions in the tropics with more than 30% of the total variance in the IA band, during the austral summer correspond to the main anomalous ENSO-related circulation centers. The 250-hPa velocity potential shows maxima in total and IS variance centered in the tropics. The IA variance is generally quite small, except over Indonesia and the eastern tropical Pacific, consistent with ENSO-related anomalies. Seasonality is evident in the variance patterns for all variables. Maximum variability is observed in the winter hemisphere for SLP and 250-hPa streamfunction and during the austral summer for OLR and 250-hPa velocity potential.

RESUMO

Variabilidade da atmosfera tropical é analisada computando-se as variâncias (total, interanual - IA, e intrasazonal - IS) de radiação de onda longa (ROL), pressão ao nível do mar (PNM), função de corrente em 250-hPa e potencial de velocidade em 250-hPa, e as porcentagens da variância total nas bandas IA e IS, para o período 1985-1994 para todas as estações e para as estações de verão e inverno austrais, separadamente. Alta variabilidade de ROL nos trópicos e subtrópicos está associada principalmente à banda IS, enquanto a variância IA máxima, observada no Pacífico equatorial central e leste, está relacionada com o El Niño-Oscilação Sul (ENOS). A variância de PNM é maior nos extratrópicos, mas o padrão da porcentagem da variância total na

banda IA mostra máximos nos trópicos consistente com os centros de ação da Oscilação Sul (OS). Uma porção substancial da variância IS na PNM está relacionada com a oscilação de Madden-Julian. A maior variância da função de corrente em 250-hPa é encontrada nos subtrópicos e baixas latitudes médias. As pequenas regiões nos trópicos com mais que 30% da variância total na banda IA, no verão austral, correspondem aos principais centros de circulação anômala relacionada ao ENOS. O potencial de velocidade em 250-hPa mostra os máximos de variâncias total e IS centrados nos trópicos. A variância IA é geralmente bem pequena, exceto sobre a Indonésia e o Pacífico tropical leste, consistente com as anomalias relacionadas com ENOS. Sazonalidade é evidente nos padrões das variâncias de todas as variáveis. Observa-se máxima variabilidade no hemisfério de inverno para PNM e função de corrente em 250-hPa e, durante o verão austral, para ROL e potencial de velocidade em 250-hPa.

1. INTRODUCTION

Planetary-scale variability of the tropical circulation is primarily associated with interannual (IA) or intraseasonal (IS) time-scale phenomena. The El Niño/Southern Oscillation (ENSO) is the most important large-scale phenomenon related to IA variations in the tropical climate (e.g., Rasmusson and Arkin, 1985). Major features of the ENSO cycle include: a large-scale exchange of tropospheric mass between the regions of the eastern Indian and southeastern Pacific oceans (Walker, 1924; Walker, and Bliss, 1932), variations in the intensity of the low-level equatorial easterlies in the Pacific, and variations of the sea surface temperature (SST) in the tropical Pacific (Bjerknes, 1966, 1969, 1972). Extremes in the ENSO cycle have been related to near-global atmospheric circulation changes (Horel and Wallace, 1981; Arkin, 1982; Karoly, 1989) and to large-scale patterns of anomalous surface temperature and precipitation in the tropics and extratropics (e.g., Ropelewski and Halpert, 1986, 1987, 1989; Halpert and Ropelewski, 1992).

A major source for large-scale IS variability in the tropics is the 30-60 day or Madden and Julian oscillation (hereafter referred to as MJO). MJOs feature an eastward propagating large-scale direct zonal circulation cell, with associated variations in the patterns of tropical convection and global-scale atmospheric circulation (e.g., Weickmann, 1983; Lau and Chan, 1985; Weickmann et al., 1985; Knutson and Weickmann, 1987; Kousky and Kayano, 1994a).

In a recent series of papers (Kayano and Kousky, 1992; Kousky and Kayano, 1994a; Kousky and Kayano, 1994b; Kayano et al., 1995) low-pass and band-pass Lanczos filters were used to isolate IA and IS variability in the tropics. In this paper we provide a more detailed analysis of the variance retained in the IA and IS bands for selected atmospheric variables, and we compare our results to previous studies on IA and IS variability.

The data and methodology are described in the next section. For each variable analyzed, the geographical distributions of the variance (total, IA and IS) and the percent of variance contained in the IA and IS bands are presented in section 3. The results are discussed in section 4.

2. DATA AND METHODOLOGY

The dataset used consists of five-day non-overlapping (pentad) means of the outgoing longwave radiation (OLR), sea level pressure (SLP), 250-hPa streamfunction and 250-hPa velocity potential, available at the Climate Prediction Center, Washington, DC. The OLR data are estimated from the radiometric measurements obtained from the NOAA operational polar-orbiting satellites (Gruber and Krueger, 1984). The OLR in the tropics serves as a measure of convection (low OLR - deep convection). The 250-hPa velocity potential and 250-hPa streamfunction are derived from the circulation data which are obtained from the National Centers for Environmental Prediction (NCEP; formally the National Meteorological Center - NMC) Global Data Assimilation System (GDAS) (Dey, 1989). These data have a spatial resolution of 2.5 degrees in latitude and longitude.

The domain of our study extends from 40°N to 40°S and the period of data is from January 1985 to December 1994, except for the SLP. The SLP is extremely sensitive to model orography and resolution, and shows considerable inhomogeneities in the historical gridded analyses. To provide the scientific community with a homogeneous dataset appropriate for studying climate variability, NCEP and the National Center for Atmospheric Research (NCAR) have collaborated in performing a reanalysis of historical data using a state-of-the-art data assimilation system (Kalnay et al., 1996). Daily-averaged SLP from the NCAR/NCEP Reanalysis for the period 1985-1993 are used in this paper to form pentad means, which are then used in the variance analysis.

All variables are temporaly filtered by using Lanczos filters (Duchon, 1979), which are the same as those used by Kousky and Kayano (1994b) in their analysis of IA and IS variability for the South American sector. (See Fig. 1 therein for the filter responses). The IA time scale variations are detected by using a low-pass filter with 97 weights and specifying a response frequency of 0.5 at a period of 180 days. The IS time scale variations are detected by using a band-pass filter with 97 weights and specifying the cutoff frequencies of 0.2 pentad^{-1} and 0.0575 pentad^{-1}.

To examine the spatial patterns of variability contained in the anomaly fields we calculated for each grid-point the variance (total, IA and IS) for each variable for all seasons, and for the southern summer (November to March) and winter (May to September) seasons, separately. In addition, we computed the percent of total variance contained in the IA and IS bands.

3. RESULTS: ALL SEASONS

a. Outgoing longwave radiation (OLR)

Figure 1 shows the variance (total, IA and IS) patterns for OLR, and the percent of total variance contained in the IA and IS bands. The largest values of total OLR variance are observed in the tropics over the Indian and western Pacific Oceans. Large values of total variance extend eastward from the western tropical Pacific in a broad band along the Intertropical Convergence Zone (ITCZ) over the eastern North Pacific, and southeastward over the central South Pacific along the South Pacific Convergence Zone (SPCZ). Large values of total variance are also found over central South America and portions of southern Africa. The South American band of maximum total variance extends southeastward along the South Atlantic Convergence Zone (SACZ).

The OLR IA variance features a single maximum in the equatorial central Pacific, while the OLR IS variance presents a pattern similar to that for the total variance, with the largest values from the central Indian Ocean eastward to the western tropical Pacific. The IS variance exceeds the IA variance throughout most of the tropics, including the region of South America near the SACZ. An exception to this pattern is found in the central and eastern equatorial Pacific, where IA variability accounts for up to 60% of the total variance.

The pattern for the percent of total variance contained in the IS band does not display a

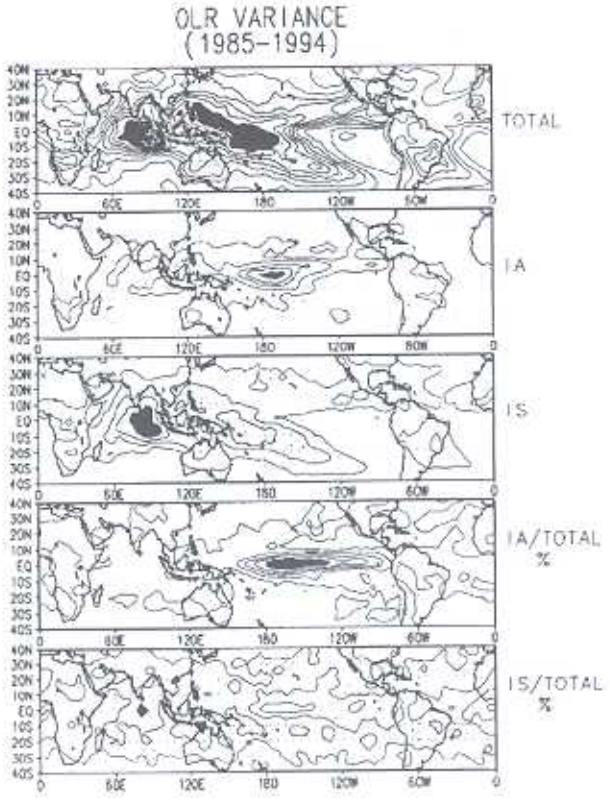

Figure 1. Outgoing longwave radiation (OLR) variance and variance ratios for the period 1985-1994. The contour interval for variance (top three panels) is 100 W² m⁻⁴. An additional contour for 50 W² m⁻⁴ has beens drawn for the IA variance. The ratios (lower two panels) are in percent with a contour interval of 10. Light (dark) shading indicates values over (400) W² m⁻⁴ for total variance, values over 200 (400) W² m⁻⁴ for IA and IS variance, and percents over 30 (50).

well-organized maximum. Instead it shows a nearly uniform pattern throughout the tropics and subtropics with values between 30 and 50%. The exception to this uniform pattern is in the central and eastern equatorial Pacific where IA variability dominates.

b. Sea level pressure (SLP)

The largest values of total, IA and IS variance for SLP (Fig. 2) are found at extratropical latitudes in both hemispheres. In the Northern Hemisphere the greatest values are found over the Pacific and Atlantic Oceans. In the Southern Hemisphere the pattern is more nearly zonally symmetric.

The percent of total variance in the IA band has maxima near 10S, 120W and over Indonesia. In both regions, which correspond to the centers of action of the Southern Oscillation, more than 30% of the total variance is contained in the IA band. In contrast, the pattern of IS variance is more uniform, with IS variability accounting for 30 to 50% of the total variance throughout most of the domain depicted.

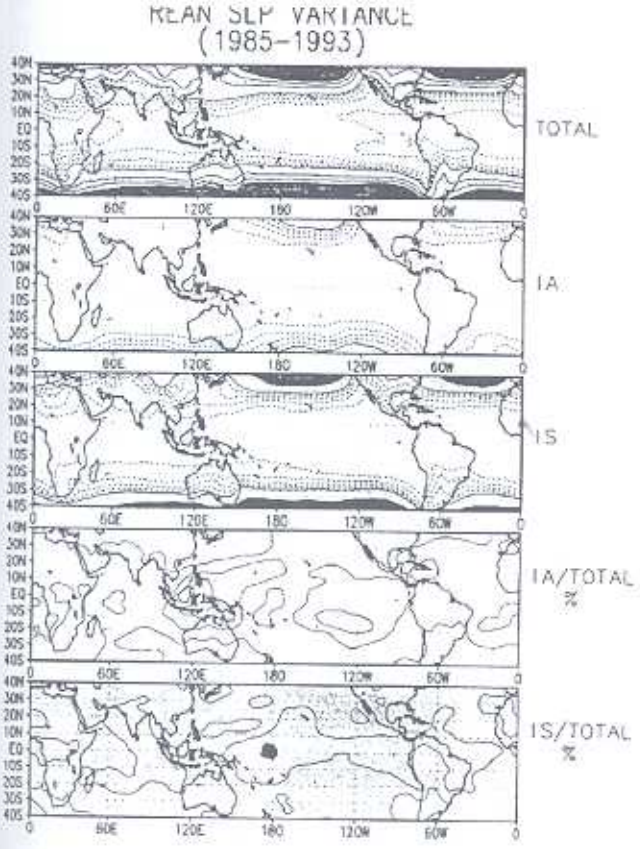

Figure 2. Sea level pressure (SLP) variance and variance ratios for the period 1985-1993). The contour interval for variance (top three panels) is 5 hPa^2 with additional contours for 1, 2, 3 and 4 hPa^2. The ratios (lower two panels) are in percent with a contour interval of 5. Light (dark) shading indicates values over 10 (20) hPa^2 for total variance, values over 5 (10) hPa^2 for IA and IS variance, and percents over 30 (50). REAN means that data are from the NCEP/NCAR reanalysis archive reanalyzed.

c. 250-hPa streamfunction

Similar to the results for SLP variance (Fig. 2), the 250-hPa streamfunction variance (total, IA and IS) patterns (Fig. 3) show considerable zonal symmetry, with the largest values found over the subtropics and midlatitudes of both hemispheres. However, in contrast to the patterns for SLP, there is less tendency for the Northern Hemisphere streamfunction variance to be concentrated over the midlatitude oceans.

IA variability generally explains less

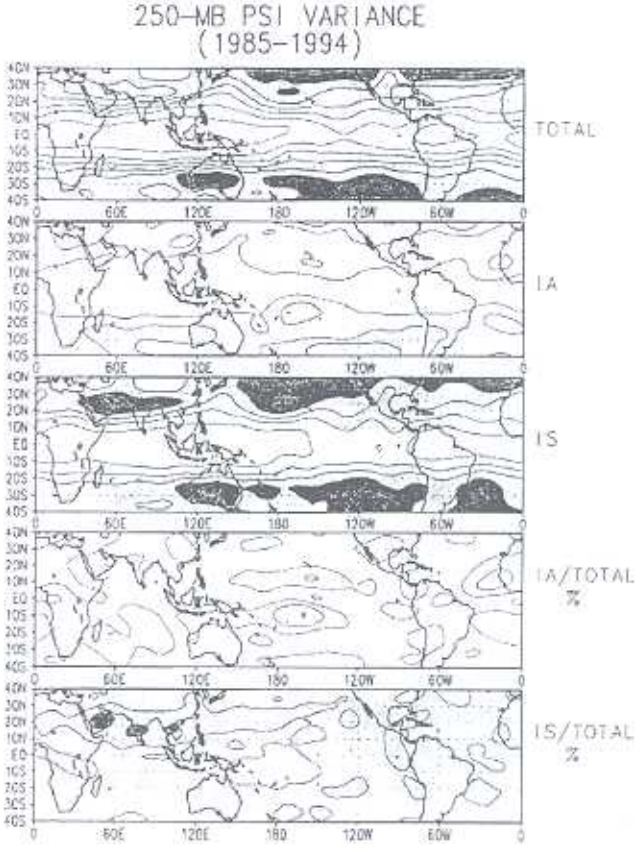

Figure 3. 250-hPa streamfunction variance and variance ratios for the period 1985-1994. The contour interval is 20 (10)x10^{12} m^4 s^{-2} for total (IA and IS) variance. The ratios (lower two panels) are in percent with a contour interval of 10. Light (dark) shading indicates values over 60 (90)x10^{12} m^4 s^{-2} for total variance, values over 5 (10)x10^{12} m^4 s^{-2} for IA and IS variance, and percents over 30 (50).

than 30% of the total variance, except over the central Pacific near 10S and 10N, and over the Atlantic near 10N. The percent of total variance in the IS band is fairly uniform over the region, with values of 30 to 50% except at low latitudes over the central Pacific where values are less than 30%.

d. 250-hPa velocity potential

The 250-hPa velocity potential variance (total, IA and IS) patterns (Fig. 4) show the largest variances in the tropics and subtropics. Maximum values of total variance are found over Indonesia, the central Pacific (in the vicinity of the SPCZ), and over northern South America. Maxima in IA variance are observed over the eastern tropical Pacific, Indonesia and central Africa. IS variance is largest over the Indian Ocean eastward to the tropical west Pacific.

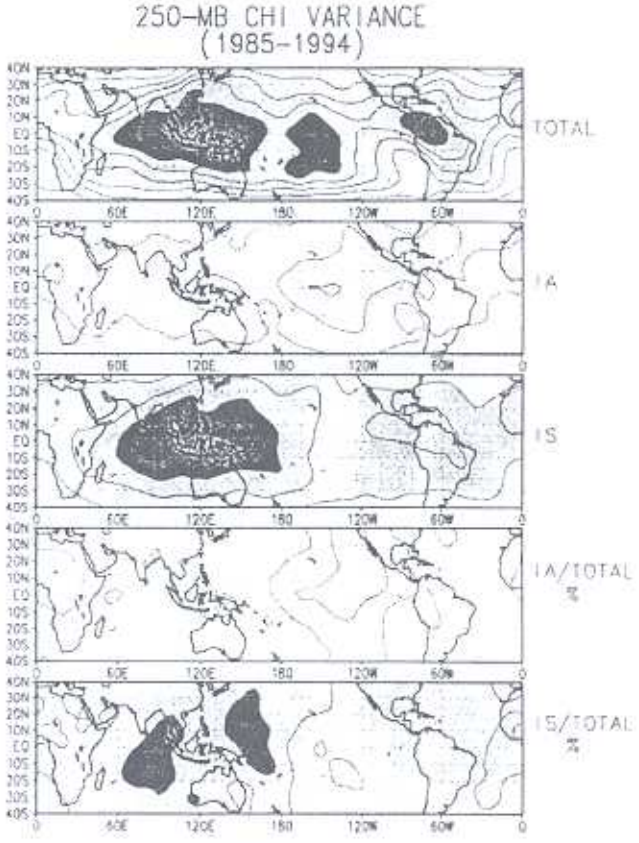

Figure 4. 250-hPa velocity potential variance and variance ratios for the period 1985-1994. The contour interval is $1x10^{12}$ m^4 s^{-2} for the variance (top three panels). The ratios (lower two panels) are in percent with a contour interval of 5. Light (dark) shading indicates values over 6 (9)$x10^{12}$ m^4 s^{-2} for total variance, values over 2 (4)$x10^{12}$ m^4 s^{-2} for IA and IS variance, and percents over 30 (50).

More than 30% of the total variance is contained in the IA band over the east-central Pacific, with smaller percentages observed throughout the remainder of the region. The percent of total variance in the IS band is more than 30% throughout nearly the entire domain, with the largest values over the central Indian Ocean and over the western Pacific.

4. SEASONAL ANALYSES

a. OLR

The total OLR variance for the southern summer (Fig. 5) and winter (Fig. 6) season is closely related to regions of intense tropical convection. During the southern summer, the variance is greatest in the areas immediately surrounding the regions of strongest convection (central Africa, Indonesia, and the Amazon Basin of South America), which are regions of relative minima in Fig. 5. Over Africa, large OLR variance is found over the southern portion of the continent (15-30S), along the east coast and just north of the equator. Large variance values extend eastward from Af-

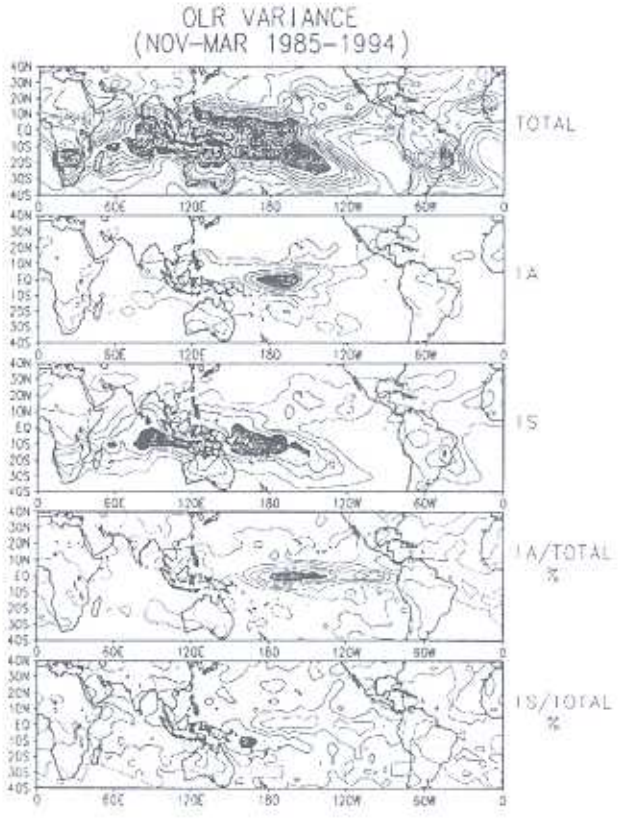

Figure 5. Same as in Fig. 1, except for southern summer (November - March).

rica to the central Pacific. From there, large values extend southeastward along the SPCZ, and northeastward to Mexico. The large values over the latter region are generally north of the mean position of the ITCZ, and are probably related to moisture plumes (McGuirk et al. 1987; McGuirk et al. 1988; Iskenderian 1995) that result from extratropical-tropical interactions. In the vicinity of South America, largest values are found over southern and eastern Brazil (including the neighboring Atlantic along the SACZ), and extending northeastward to the west coast of Africa, in a similar way as for the eastern Pacific.

During the southern winter (Fig. 6) the largest OLR variance is found over the central Indian and west Pacific Oceans. Large values of OLR variance are also observed throughout the central and eastern North Pacific along the ITCZ, over the Caribbean Sea and Central America, over southeastern South America, and over the South Pacific from the Solomon Islands southeastward to midlatitudes.

The pattern of IA variance for both seasons presents maximum values (largest during the

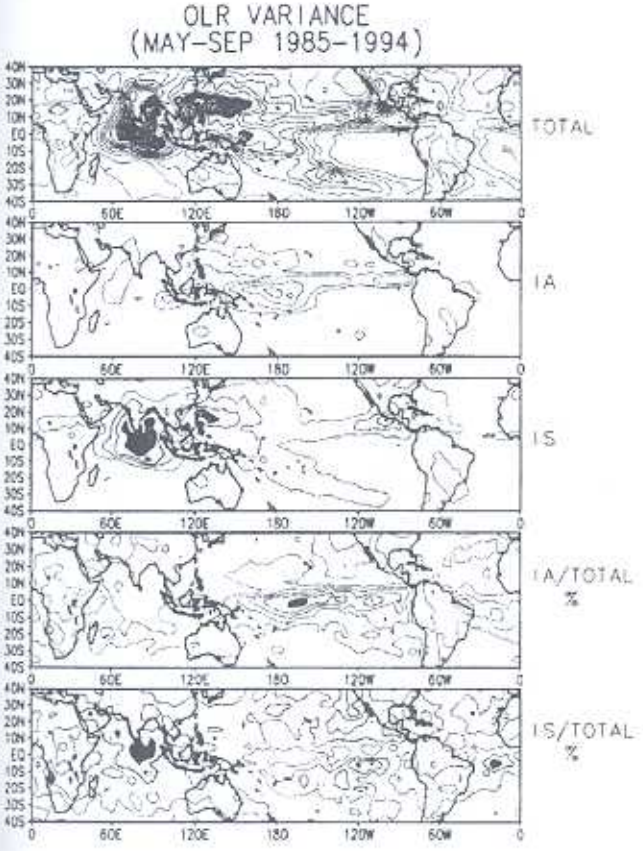

Figure 6. Same as in Fig. 1, except for southern winter (May - September).

southern summer) over the central equatorial Pacific. The IA variance maximum in the central Pacific, just east of the date line during austral summer and just west of the date line during austral winter, contains more than 50% of the total variance. The maximum percent of the total variance contained in the IA band over the coastal areas of the northern Northeast Brazil during the reflects austral winter, partially reflects the results obtained by Rao and Hada (1990), who analyzed the connections between the southern oscillation and seasonal rainfall over Brazil.

The IS variance shows quite different patterns for the two seasons. During the southern summer, high values extend from southern Africa eastward across Indonesia and northern Australia to the central Pacific. Also, there is a small region of high variance over eastern Brazil. In contrast, during the southern winter OLR IS variance is rather weak throughout the western hemisphere, except for the region just west of Central America. The largest values are observed over the northern Indian Ocean and over the southwestern North Pacific. The patterns for the percent of total variance contained in the IS band are similar for both seasons.

b. SLP

The SLP variance (total, IA and IS) (Figs. 7 and 8) is greatest in the midlatitudes, especially in the winter hemisphere. Within the tropics and subtropics IA variability accounts for more than 30% of the total variance over the southern Philippines and Indonesia during the southern summer, and over southern Indonesia and the eastern tropical Pacific during the southern winter. For the remainder of the tropics less than 30% of the total variance is contained in the IA band. In both seasons more than 30% of the total variance is contained in the IS band throughout most of the tropics and subtropics. Values exceed 50% over portions of the tropical Pacific and Indian Oceans.

It is noteworthy that over South America there is considerably more IS variance during the austral winter than during the summer, especially just east of the Andes and slong the east coast north of 30 S. This IS signal in the SLP reflects cold air incursions over South America during the winter, which agrees with the results of Kousky and Ferreira (1981), who documented the spatial distribution of the surface pressure fluctuations over Bra-

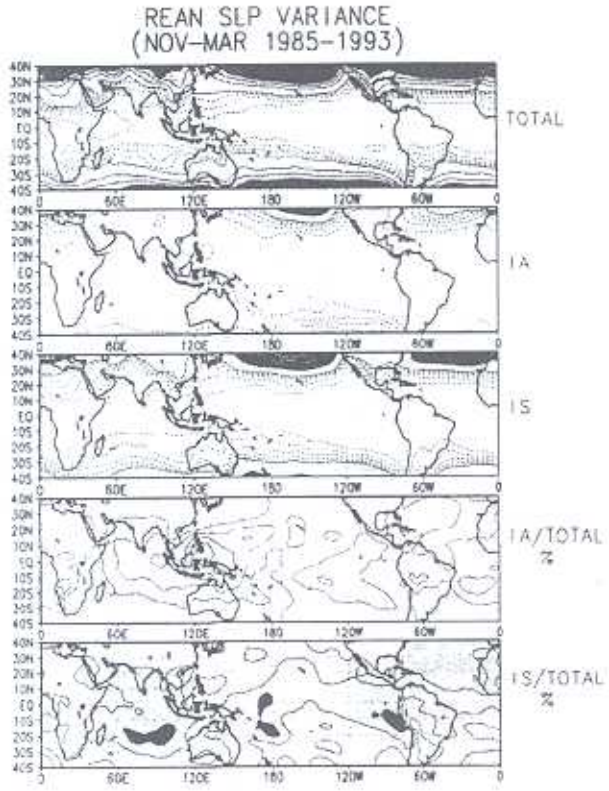

Figure 7. Same as in Fig. 2, except for southern summer (November - March).

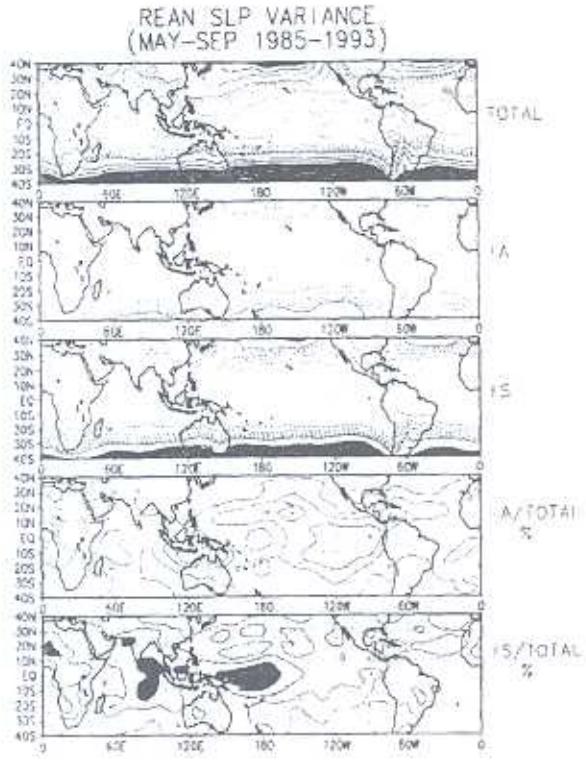

Figure 8. Same as in Fig. 2, except for southern winter (May - September).

zil. Based on principal component analysis of daily station pressure data for 1968 with the annual mean and first two harmonics of the annual cycle removed, they found a pattern with the greatest pressure variations in southern and western Brazil. They related this pattern to incursions of cold air during winter.

Furthermore, the IS variance analyses emphasize the role played by the central plateau (Planalto Central) in the winter incursion of cold air masses in deflecting them. This orographic effect is confirmed by the reduced IS variance observed over the central Plateau during the austral winter. Similar patterns but weaker are also observed over Africa and Australia.

c. 250-hPa streamfunction

Total and IS 250-hPa streamfunction variance are greatest in the midlatitudes of both hemispheres (Figs. 9 and 10). In contrast, the IA variance has some maxima in the subtropics as well as in the extratropics. The subtropical centers of maximum IA variance in the central Pacific during summer are well defined and located to the north and south of the center of maximum OLR IA

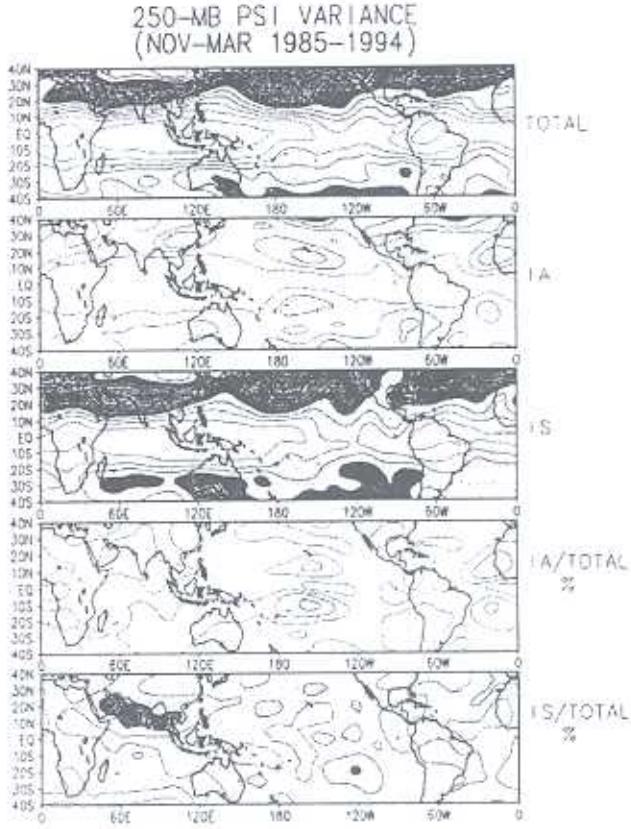

Figure 9. Same as in Fig. 3, except for southern summer (November - March).

variance. During the winter, the centers of maximum 250-hPa streamfunction in the subtropical central Pacific are not well defined, but there are indications that they are located to the south and to the northwest of the maximum OLR IA variance.

The patterns of total and IS variance show more seasonal variability in the Northern Hemisphere than in the Southern Hemisphere. Many regions of the Southern Hemisphere have substantial variance in the IA band during both seasons, whereas IA variance in the Northern Hemisphere is

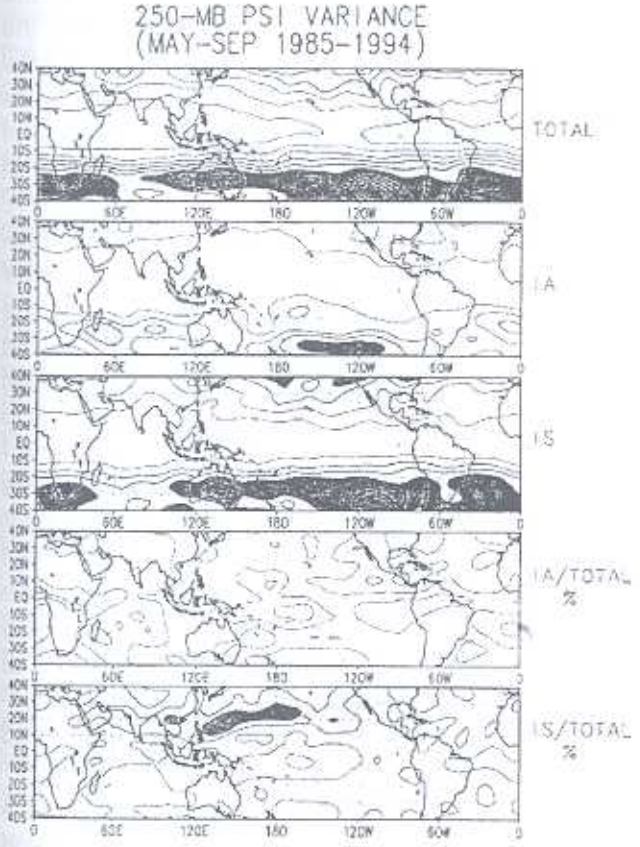

Figure 10. Same as in Fig. 3, except for southern winter (May - September).

large mainly during the southern summer. Only a few regions in the tropics and subtropics have more than 30% of the total variance contained in the IA band. The percent of total variance contained in the IS band is greatest (more than 50%) in the northern subtropics over India and Southeast Asia during the southern summer and over the western and central North Pacific during the southern winter. Most of the remainder of the tropics and subtropics has values greater than 30%.

d. 250-hPa velocity potential

The patterns of total and IS variance for 250-hPa velocity potential are quite similar, especially during the southern summer (Fig. 11). The IS band accounts for more than 50% of the total variance over a large portion of the tropics from Africa eastward to the western Pacific during the southern summer. During the southern winter (Fig. 12) more than 50% of the total variance is contained in the IS band over the western Pacific and Southeast Asia, and over Central America and the western

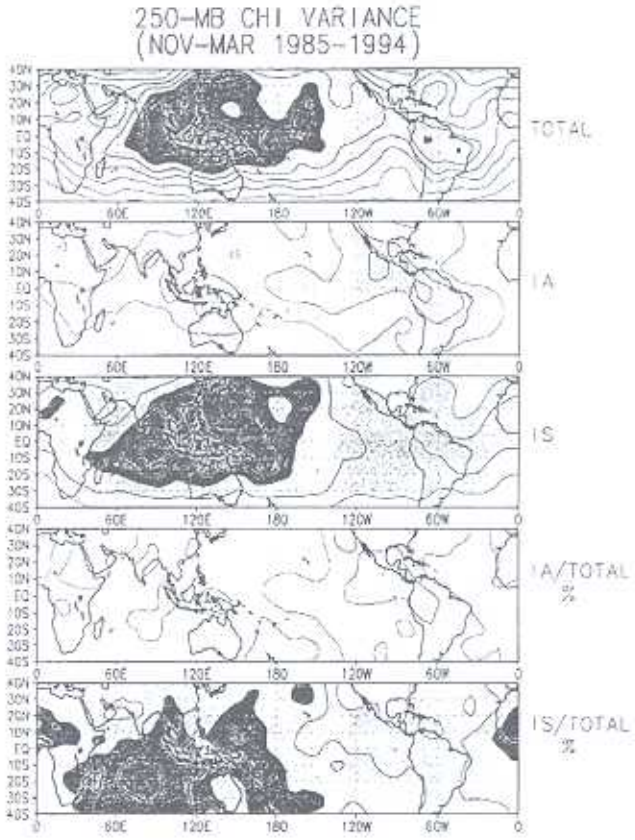

Figure 11. Same as in Fig. 4, except for southern summer (November - March).

Atlantic. Also evident in the patterns of IS variance is a seasonal shift of the maximum percentages into the summer hemisphere. The IS variance is generally greater than the IA variance, except over the central tropical Pacific during the southern winter and over portions of Central America during the southern summer.

5. DISCUSSION AND CONCLUSION

Large values of total OLR variance are located in tropical and subtropical regions where intense deep convection is common. High values are found across the tropics from the Indian Ocean

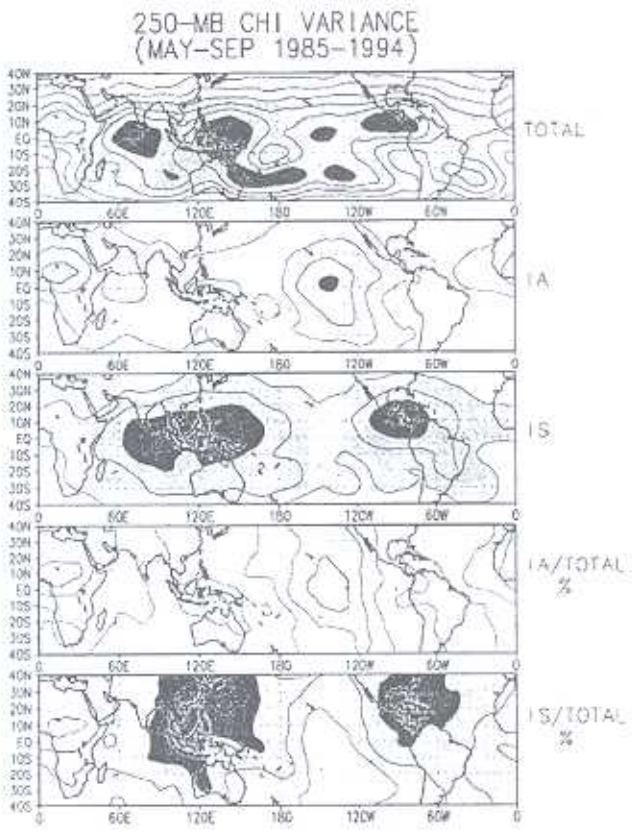

Figure 12. Same as in Fig. 4, except for southern winter (May - September).

eastward to the western Pacific and extending southeastward to the subtropics and northeastward to the tropical North Pacific. The southeast extension coincides with the location of the SPCZ and the northeast extension is close to the position of the ITCZ. In addition, high values are found over southeast South America and the adjacent Atlantic Ocean, which coincides with the SACZ.

Much of this variance is associated with IS variability. In contrast, the maximum IA OLR variance is observed in the equatorial central and eastern Pacific, which is an area that experiences large IA variability related to ENSO. In this area approximately 50% of the total OLR variance is found in the IA band. The ENSO-related variations in the convection in this region are closely tied to IA variations in the sea surface temperature (SST), such that above (below) normal SST occurs with enhanced (reduced) convection during warm (cold) episodes (e.g., Rasmusson and Arkin 1985).

Despite the similarities between the maps of the OLR total and IS variance, indicating the important role played by the IS time scale phenomena in determining the OLR total variability, the IS band accounts for only approximately 30% of the total variance over most of the study domain. The strong IS variability in OLR, observed in the Indian and equatorial western Pacific Oceans, has been related to the MJO (e.g., Weickmann 1983; Lau and Chan 1985), as has the IS variability in the regions of the SPCZ and SACZ (Weickmann at al. 1985; Casarin and Kousky 1986; Kousky and Cavalcanti 1988). The relatively weak IS variability over the equatorial central and eastern Pacific has been noted previously (Knutson and Weickmann 1987).

The SLP variance is largest in the extratropics, with relatively weak variance in the tropics. However, the pattern of percent of total variance contained in the IA band shows maxima that correspond well with the centers of action of the Southern Oscillation. These centers vary in intensity and position depending on the season. During the southern summer the centers of maximum percent are found over Indonesia and over the south-central Pacific near Tahiti. During the southern winter the Indonesian center is somewhat smaller and weaker, and the center in the Pacific is larger and shifted east and north with respect to the position observed during the southern summer. Approximately 30% of the total SLP variance near Hawaii is contained in the IA band during this season. The IS band accounts for over 30% of the total SLP variance in most of the tropics, with higher percentages over the Indian and central Pacific Oceans. A substantial portion of the IS variance in SLP is related to the eastward propagating MJO (Madden and Julian, 1972; Kousky and Kayano, 1994a).

The greatest variance of the 250-hPa streamfunction is found in the subtropics and lower midlatitudes. IA variance is rather weak, with only small regions having more than 30% of the total variance in this band. However, during the southern summer those regions correspond to the main anomalous circulation centers observed during extremes in the Southern Oscillation; anomalous anticyclonic (cyclonic) couplet over the central Pacific and anomalous cyclonic (anticyclonic) couplet over the Atlantic during warm (cold) episodes (Bjerknes 1969; Arkin 1982; Rasmusson and Arkin 1985; Kousky and Ropelewski 1989).

The largest percent of total streamfunction variance in the IS band (>50%) is found near 20N in a zonal band from Saudi Arabia

eastward to Southeast Asia, during the southern summer, and in a zonal band from Southeast Asia to the Hawaiian Islands during the southern winter. These regions have been found to have considerable variability in 10-day low-pass filtered 250-hPa streamfunction data (Hsu and Lin 1992), which is included in our IS filtered data.

The 250-hPa divergent circulation, represented by the velocity potential, has the largest spatial extent for the variables analyzed in this paper. Maxima in total and IS variance are centered in the tropics. The total variance is maximum over Indonesia, the eastern Indian Ocean and the western Pacific, which is also the primary region of deep tropical convection and upper tropospheric divergence within the tropics (e.g., Arkin et al., 1986). Considerable variance is also found over northern South America. The IA variance is generally quite small, except over Indonesia and the eastern tropical Pacific where the IA band accounts for more than 30% of the total variance. This pattern is consistent with ENSO-related anomalies. During warm episodes the anomalous circulation over the equatorial central and eastern Pacific features anomalous upper tropospheric divergent flow associated with the enhanced convection and abnormally warm waters (e.g., Rasmusson and Arkin, 1985).

In general, a considerably larger proportion of the total velocity potential variance is contained in the IS band, particularly in the eastern Hemisphere, where over 40% of the total variance is in this band. This variance is primarily related to MJO activity (Knutson and Weickmann, 1987; Kousky and Kayano, 1994a).

Seasonality is evident in the SLP and 250-hPa streamfunction variance patterns, with maximum variance in the winter hemisphere. The seasonal differences in the OLR and velocity potential variability are more pronounced in the tropics. Both variables display greater variance during the southern summer when ENSO-related IA variability and MJO-related IS variability are strongest (e.g., Rasmusson and Arkin, 1985; Kousky and Kayano, 1994a).

Our patterns of the percent of total variance for both the IA and IS bands are consistent with previous studies in which empirical orthogonal functions have been used to determine the primary patterns associated with interannual and intraseasonal variability (e.g., Weickmann, 1983; Knutson and Weickmann, 1987; Mo and Kousky, 1993; Kousky and Kayano, 1994a, 1994b). In addition, we have documented the seasonality related to both IS and IA variability for selected tropospheric variables.

6. ACKNOWLEDGMENTS

This research was initiated during a visit by the first author to the National Meteorological Center/ Climate Analysis Center (presently the National Centers for Environmental Prediction/ Climate Prediction Center) under the sponsorship of the University Corporation for Atmospheric Research, during 1992-93. The first author is partially supported by project number 300033/94-0 under the sponsorship of the Conselho Nacional de Desenvolvimento Cientifico e Tecnológico.

7. REFERENCES

Arkin, P. A., 1982: The relationship between interannual variability in the 200 mb tropical wind field and the Southern Oscillation. Mon. Wea. Rev., 110, 1393-1404.

Arkin, P. A., V. E. Kousky, J. E. Janowiak, and E. A. O'Lenic, 1986: Atlas of the tropical and subtropical circulation derived from National Meteorological Center Operational Analyses, NOAA Atlas 7, 96pp., Natl. Oceanic Atmos. Admin., Silver Spring, MD.

Bjerknes, J., 1966: A possible response of the atmospheric Hadley circulation to equatorial anomalies of ocean temperature. Tellus, 18, 820-829.

Bjerknes, J., 1969: Atmospheric teleconnections from the equatorial Pacific. Mon. Wea. Rev., 97,163-172.

Bjerknes, J., 1972: Large-scale atmospheric response to the 1964-65 Pacific equatorial warming. J. Phys. Oceanogr., 2, 212-217.

Casarin, D. P., and V. E. Kousky, 1986: Anomalias de precipitação no sul do Brasil e variações na circulação atmosférica. Rev. Bras. Meteor., 1, 86-90.

Dey, C. H., 1989: The evolution of objective analysis methodology at the National Meteorological Center. Wea. Forecasting, 4, 297-312.

Duchon, C. E., 1979: Lanczos filtering in one and

two dimensions. J. Appl. Meteor., 18, 1016-1022.

Gruber, A., and A. F. Krueger, 1984: The status of the NOAA outgoing longwave radiation data set. Bull. Amer. Meteo. Soc., 65, 958-962.

Halpert, M. S., and C. F. Ropelewski, 1992: Surface temperature patterns associated with the Southern Oscillation. J. Climate, 5, 577-593.

Horel, J. D., and J. M. Wallace, 1981: Planetary scale atmospheric phenomena associated with the Southern Oscillation. Mon. Wea. Rev., 109, 813-829.

Hsu, H-H, and S-H. Lin, 1992: Global teleconnections in the 250-mb streamfunction field during the Northern Hemisphere winter, Mon. Wea. Rev., 120, 1169-1190.

Iskenderian, H., 1995: A 10-year climatology of Northern Hemisphere tropical cloud plumes and their composite flow patterns. J. Climate, 8, 1630-1637.

Kalnay E., M. Kanamitsu, R. Kistler, W. Collins, D.Deaven, L. Gandin, M. Iredell, S. Saha, G. White, J. Woolen, Y. Zhu, M. Chelliah, W. Ebisuzaki, W. Higgins, J. Janowiak, K. C. Mo, C. Ropelewski, J. Wang, A. Leetmaa, R. Reynolds, R. Jenne and D. Joseph, 1996: The NCEP/NCAR 40-year Reanalysis Project. Bull. American Meteor. Soc., 77, 437-471.

Karoly, D. J., 1989: Southern Hemisphere circulation features associated with El Niño-Southern Oscillation events. J. Climate, 2, 1239-1252.

Kayano, M. T., and V. E. Kousky, 1992: Sobre o monitoramento das oscilações intrasazonais. Rev. Bras. Meteor., 7, 593-602.

Kayano, M. T., V. E. Kousky and J. E. Janowiak, 1995: Outgoing longwave radiation biases and their impacts on empirical orthogonal function modes of interannual variability in the tropics. J. Geophys. Res., 100, 3173-3180.

Knutson, T. R., and K. M. Weickmann, 1987: 30-60 day atmospheric oscillations: composite life cycles of convection and circulation anomalies. Mon. Wea. Rev., 117, 1407-1436.

Kousky, V. E., and I. F. A. Cavalcanti, 1988: Precipitation and atmospheric circulation anomaly patterns in the South American sector. Rev. Bras. Meteor., 3, 199-206.

Kousky, V. E., and N. J. Ferreira, 1981: Interdiurnal surface pressure variations in Brazil: their spatial distributions, origins and effects. Mon. Wea. Rev., 109, 1999-2008.

Kousky, V. E., and M. T. Kayano, 1994a: Real-time monitoring of intraseasonal oscillations. Proceedings of the Eighteenth Annual Climate Diagnostics Workshop, 1-5 November 1993, Boulder, CO, 66-69.

Kousky, V. E., and M. T. Kayano, 1994b: Principal modes of outgoing longwave radiation and 250-mb circulation for the South American sector. J. Climate, 7, 1131-1143.

Kousky, V. E., and C. F. Ropelewski, 1989: Extremes in the Southern Oscillation and their relationship to precipitation anomalies with emphasis on the South American region. Rev. Bras. Meteor., 4, 351-363.

Lau, K-M., and P. H. Chan, 1985: Aspects of the 40-50 day oscillation during the Northern winter as inferred from outgoing longwave radiation. Mon. Wea. Rev., 113, 1889-1909.

Madden, R. A., and P. R. Julian, 1972: Description of global-scale circulation cells in the tropics with a 40-50 day period. J. Atmos. Sci., 29, 1109-1123.

McGuirk, J. P., A. H. Thompson, and N. R. Smith, 1987: Moisture bursts over the tropical Pacific Ocean. Mon. Wea. Rev., 115, 787-798.

McGuirk, J. P., A. H. Thompson and J. R. Schaffer, 1988: An eastern Pacific tropical plume. Mon. Wea. Rev., 116, 2505-2521.

Mo, K. C., and V. E. Kousky, 1993: Further analysis of the relationship between circulation anomaly patterns and tropical convection. J. Geophys. Res., 98, 5103-5113.

Rasmusson, E. M., and P. A. Arkin, 1985: Interannual climate variability associated with the El Niño/Southern Oscillation. In: J. C. J. Nihoul (Editor), Coupled-Ocean Atmosphere Models, Elsevier, Amsterdam, 289-302.

Rao, V. B., and K. Hada, 1990: Characteristics of rainfall over Brazil: annual variations and connections with the Southern Oscillation. Theor. Appl. Climatol., 42, 81-91.

Ropelewski, C. F., and M. S. Halpert, 1986: North

American precipitation and temperature patterns associated with the El Niño/Southern oscillation (ENSO). Mon. Wea. Rev., 114, 2352-2362.

Ropelewski, C. F., and M. S. Halpert, 1987: Global and regional scale precipitation patterns associated with the El Niño/Southern Oscillation. Mon. Wea. Rev., 115, 1606-1626.

Ropelewski, C. F., and M. S. Halpert, 1989: Precipitation patterns associated with the high index phase of the Southern Oscillation. J. Climate, 2, 268-284.

Walker, G. T., 1924: Correlation in seasonal variations of weather IX. A further study of the world weather. Mem. Indian Meteor. Dept., 24, 275-332.

Walker, G. T., and E. W. Bliss, 1932: World Weather V. Mem. Roy. Meteor. Soc., 4, 53-84.

Weickmann, K. M., 1983: Intraseasonal circulation and outgoing longwave radiation modes during northern winter. Mon. Wea. Rev., 111, 1838-1858.

Weickmann, K. M., G. R. Lussky and J. E. Kutzbach, 1985: A global-scale analysis of intraseasonal fluctuations of outgoing longwave radiation and 250-mb stream function during the northern winter. Mon. Wea. Rev., 113, 941-961.